# Single Inclusive $\pi^{\pm}$ and $K^{\pm}$ Production in $e^+e^-$ Annihilation at Center-of-Mass Energies from 2.000 to 3.671 GeV

M. Ablikim *et al.*[*]
(BESIII Collaboration)

(Received 24 February 2025; revised 5 July 2025; accepted 11 September 2025; published 8 October 2025)

Using data samples with a total integrated luminosity of 253 $\mathrm{pb}^{-1}$ collected by the BESIII detector operating at the BEPCII collider, the differential cross sections of inclusive $\pi^{\pm}$ and $K^{\pm}$ production, as a function of the momentum and normalized by the total hadronic cross section, are measured at center-of-mass energies from 2.000 to 3.671 GeV. The measured $\pi^{\pm}$ cross sections are consistent with the previously reported $\pi^0$ cross sections by BESIII, while the $K^{\pm}$ cross sections are systematically higher than the $K^0_S$ cross sections by a factor of approximately 1.4. These new results are in agreement with state-of-the-art QCD analyses at next-to-next-to-leading-order accuracy, particularly in the large hadron momentum region at energy scales down to 3 GeV. These findings support the validity of isospin symmetry in parton fragmentation processes.

DOI: 10.1103/5kxw-3mbw

Single inclusive hadron production in electron-positron annihilation (SIA) provides direct insights into the hadronization process in a controlled and clean environment. It enhances our understanding of how quarks and gluons fragment into hadrons, which is crucial for advancing our knowledge of quantum chromodynamics (QCD) and for accurately modeling hadron production in various high-energy processes. The typical experimental observable in SIA is

$$\frac{1}{\sigma(e^+e^- \to \text{hadrons})}\frac{d\sigma(e^+e^- \to h + X)}{dp_h}, \qquad (1)$$

where $\sigma(e^+e^- \to \text{hadrons})$ is the cross section for $e^+e^-$ annihilation to all possible hadronic final states (referred to as inclusive hadronic events hereafter), $p_h$ represents the momentum of the identified hadron $h$, $X$ refers to everything else. This observable in high-energy collisions can be factorized using the QCD factorization theorem [1], which allows it to be expressed as a convolution of perturbative hard-part coefficients and nonperturbative fragmentation functions (FFs). At leading order in $\alpha_s$, this observable can be interpreted as $\Sigma_q e_q^2[D_q^h(z,\mu) + D_{\bar{q}}^h(z,\mu)]$, where $e_q$ is the fractional charge of the quark $q$, and $D^h_{q/\bar{q}}(z,\mu)$ is the FF presenting the probability density that an outgoing parton (quark $q$ or antiquark $\bar{q}$) produces a hadron $h$. The parameter $\mu$ is the factorization scale, typically chosen to be the center-of-mass (c.m.) energy $\sqrt{s}$. The dimensionless variable $z \equiv 2\sqrt{p_h^2c^2 + M_h^2c^4}/\sqrt{s}$ denotes the relative energy of hadron $h$ with mass $M_h$.

In $e^+e^-$ collisions, a broad range of measurements is available for the single inclusive production of identified light charged hadrons, including $\pi^{\pm}$, $K^{\pm}$, $p/\bar{p}$, as well as unidentified charged hadrons, which have been summarized comprehensively, e.g., in Table IV of Ref. [2]. These measurements are primarily concentrated in the higher-energy region. The Belle [3,4] and *BABAR* [5] Collaborations have performed precision measurements at around 10.5 GeV. In the energy region below 10 GeV, the only available measurements of inclusive $\pi^{\pm}/K^{\pm}$ production come from the DASP experiment [6] conducted in 1978, mainly focusing on the contribution of charm to charged hadron production near the charm threshold. However, there is a gap in measurements at lower-energy scales, especially in the continuum region 2–3 GeV. In this Letter, we present a study of the processes $e^+e^- \to \pi^{\pm}/K^{\pm} + X$ using datasets collected at eight c.m. energies from 2.000 to 3.671 GeV, with $z$ coverage from 0.13 to 0.95 and from 0.30 to 0.95 for $\pi^{\pm}$ and $K^{\pm}$, respectively. The results provide a unique opportunity to test QCD factorization at low-energy scales and to assess the consistency of charged hadron production between $e^+e^-$ collisions and semi-inclusive deep inelastic scattering measurements from COMPASS [7], HERMES [8], and Jefferson Lab [9]. Furthermore, with a variety of identified final-state hadrons, it allows for the exploration of intriguing QCD phenomena, such as testing isospin symmetry. In particular, recent comparisons of the yields of $K^0_S$ and $K^{\pm}$ in

---

[*] Full author list given at the end of the Letter.

high-energy nuclear collisions suggest potential violations of isospin symmetry, which contradicts the conclusions derived from mass measurements of these particles [10]. The SIA process, as the cleanest process to detect particle productions, provides a unique and precise probe for investigating such fundamental effects and clarifying the role of isospin symmetry in the parton fragmentation processes.

The datasets used in this Letter were collected with the BESIII detector [11] running at BEPCII [12]. Experimentally, the normalized differential cross section for the inclusive production of the identified $\pi^\pm/K^\pm$ in Eq. (1) is determined with

$$\frac{N^{\mathrm{obs}}_{\pi^\pm/K^\pm}}{N^{\mathrm{obs}}_{\mathrm{had}}}\frac{1}{\Delta p}f_{\pi^\pm/K^\pm}, \tag{2}$$

where $N^{\mathrm{obs}}_{\pi^\pm/K^\pm}$ is the number of $e^+e^- \to \pi^\pm/K^\pm + X$ events within a certain momentum range $\Delta p$ (referred to as the momentum bin hereafter), $N^{\mathrm{obs}}_{\mathrm{had}}$ represents the number of observed hadronic events in the $e^+e^-$ annihilation at a given c.m. energy, and $f_{\pi^\pm/K^\pm}$ is the correction factor accounting for the detection efficiency and initial-state radiation effects.

To identify the signal events, the inclusive hadronic events are first selected [13]. The dominant background processes $e^+e^- \to e^+e^-$ (Bhabha scattering) and $e^+e^- \to \gamma\gamma$ are rejected by applying dedicated requirements on the showers recorded by the electromagnetic calorimeter. In the remaining events, a set of selection criteria are implemented to identify the good charged tracks (prongs). Events with zero or one prong are removed to suppress the contribution of quantum-electrodynamics (QED) related and beam-associated backgrounds. For events with two or three prongs, further requirements are employed to suppress QED-related backgrounds. Events with more than three prongs are regarded as hadronic events directly. More details of the selection of inclusive hadronic events are described in Ref. [13].

Although comprehensive selection criteria have been used to select the inclusive hadronic events, residual background still exists in the data. The yields of residual QED-related background events are estimated by analyzing the corresponding Monte Carlo (MC) simulation samples, which are produced based on the Geant4 software [14]. In these simulations, the geometric description of the BESIII detector and its interaction with particles are implemented. The background processes $e^+e^- \to e^+e^-$, $\mu^+\mu^-$, and $\gamma\gamma$ are generated by the BABAYAGA3.5 tool [15]. At $\sqrt{s} = 3.671$ GeV, which is above the threshold of $\tau^+\tau^-$ pair production, the $e^+e^- \to \tau^+\tau^-$ process is simulated with the KKMC program [16], and the decay of the $\tau$ lepton is modeled by EvtGen [17,18]. The two-photon processes $e^+e^- \to e^+e^-X$ with $X = e^+e^-(\mu^+\mu^-)$, $\eta(\eta')$, and $\pi^+\pi^-(K^+K^-)$ are simulated using the generators DIAG36 [19], EKHARA [20], and GALUGA2.0 [21], respectively. In addition, the beam-associated background is estimated with a sideband method developed in Ref. [13]. A variable $V_z^{\mathrm{evt}}$ representing the average vertex position along the beam direction of all charged tracks is used to estimate the beam-associated background, with events in the sideband region of $V_z^{\mathrm{evt}}$ assumed to be beam associated.

Table I summarizes the integrated luminosities, the number of total selected inclusive hadronic events ($N^{\mathrm{tot}}_{\mathrm{had}}$), and the total remaining background events ($N_{\mathrm{bkg}}$) at each c.m. energy, where $N^{\mathrm{obs}}_{\mathrm{had}} = N^{\mathrm{tot}}_{\mathrm{had}} - N_{\mathrm{bkg}}$.

From the inclusive hadronic events, the $\pi^\pm/K^\pm$ mesons are selected with the particle identification (PID), which combines the measurements of the specific ionization energy loss in the multilayer drift chamber (MDC) and the flight time from interaction point to the time-of-flight counter to form the probability $\mathcal{P}(h)(h = \pi, K, p)$ under each hadron hypothesis. The charged track is identified as the hadron species resulting in the highest probability. Because of the misidentification effect, the raw counts ($N^{\mathrm{raw}}_{h^\pm}$) obtained after applying the PID requirements and subtracting the normalized numbers of remaining background tracks in each momentum bin are written as

$$N^{\mathrm{raw}}_{h^\pm} = \sum_{g=\pi,K,p} \epsilon_{g^\pm\to h^\pm} N^{\mathrm{obs}}_{g^\pm}, \tag{3}$$

where $N^{\mathrm{obs}}_{g^\pm}$ is the number of hadron $g^\pm$ free of misidentification. The $\epsilon_{g^\pm\to h^\pm}$ terms stand for the particle identification ($g = h$) or misidentification ($g \neq h$) efficiencies, which constitute a PID efficiency matrix. Accordingly, the transition from the raw counts to the observed counts requires the inversion of the PID efficiency matrix. In our Letter, the contamination of the electron or muon to $\pi/K$ sample is strongly suppressed due to the selection criteria of hadronic events and is therefore neglected. Nevertheless, these contributions are considered in the systematic uncertainty study. In addition, the misidentifications from the oppositely charged hadrons are ignored due to the corresponding low efficiencies.

The PID efficiencies are studied using the $\pi^\pm$ control sample via $J/\psi \to \pi^+\pi^-\pi^0$, $K^\pm$ via $J/\psi \to K^0_S K^\pm \pi^\mp$, and

TABLE I. The integrated luminosities and the numbers of total selected hadronic and residual background events in different c.m. energies.

| $\sqrt{s}$ (GeV) | $\mathcal{L}$ (pb$^{-1}$) | $N^{\mathrm{tot}}_{\mathrm{had}}$ | $N_{\mathrm{bkg}}$ |
|---|---|---|---|
| 2.0000 | 10.074 | 350 298 ± 592 | 8722 ± 94 |
| 2.2000 | 13.699 | 445 019 ± 668 | 10 737 ± 104 |
| 2.3960 | 66.869 | 1 869 906 ± 1368 | 47 550 ± 219 |
| 2.6444 | 33.722 | 817 528 ± 905 | 210 42 ± 146 |
| 2.9000 | 105.253 | 2 197 328 ± 1483 | 56 841 ± 239 |
| 3.0500 | 14.893 | 283 822 ± 533 | 7719 ± 88 |
| 3.5000 | 3.633 | 62 670 ± 251 | 1691 ± 42 |
| 3.6710 | 4.628 | 75 253 ± 275 | 6461 ± 81 |

the proton via $J/\psi, \psi(3686) \to p\bar{p}\pi^+\pi^-$. To avoid possible bias introduced by the difference between the signal and control samples, the PID efficiencies are evaluated, and the corresponding $N^{\mathrm{obs}}_{g^\pm}$ are extracted in each momentum versus ten bins in $\cos\theta$ bin $(p, \cos\theta)$, where $\theta$ is the polar angle with respect to the symmetry axis of the MDC. The contributions to $N^{\mathrm{raw}}_{\pi^\pm/K^\pm}$ from the residual QED-related and beam-associated backgrounds are subtracted. The dominant background contribution is from Bhabha events, which is at most 10% in a few bins [22] and negligible in the other bins. The number of observed $\pi^\pm/K^\pm$ in each momentum bin is obtained by summing over all the $\cos\theta$ bins, i.e.,

$$N^{\mathrm{obs}}_{\pi^\pm/K^\pm}(i) = \sum_{j=1}^{10} N^{\mathrm{obs}}_{\pi^\pm/K^\pm}(i,j), \tag{4}$$

where $N^{\mathrm{obs}}_{\pi^\pm/K^\pm}(i)$ is the number of observed $\pi^\pm/K^\pm$ in the $i$th momentum bin, and $N^{\mathrm{obs}}_{\pi^\pm/K^\pm}(i,j)$ is that in the $i$th momentum and $j$th $\cos\theta$ bin.

The inclusive hadronic events are simulated with the LUARLW generator [13,23,24], in which, among others, the signal processes $e^+e^- \to \pi^\pm/K^\pm + X$ are included. A detailed comparison between the MC sample and the experimental data shows that the LUARLW model can reasonably describe the kinematic distributions of signal events in the data. The correction factor $f_{\pi^\pm/K^\pm}$ can be written as

$$f_{\pi^\pm/K^\pm} = \frac{\bar{N}^{\mathrm{tru}}_{\pi^\pm/K^\pm}(\mathrm{off})}{\bar{N}^{\mathrm{tru}}_{\mathrm{had}}(\mathrm{off})} \Big/ \frac{\bar{N}^{\mathrm{obs}}_{\pi^\pm/K^\pm}(\mathrm{on})}{\bar{N}^{\mathrm{obs}}_{\mathrm{had}}(\mathrm{on})}, \tag{5}$$

where the variable $\bar{N}$ denotes the number of events determined from the inclusive hadronic MC sample, either after the detector reconstruction, similar to the experimental data, with superscript "obs" or at truth level with superscript "tru." The terms "on" and "off" in the parentheses indicate that the corresponding quantities are extracted from the inclusive hadronic MC sample with or without simulating the initial-state radiation process, respectively. To avoid misidentification in the determination of $N^{\mathrm{obs}}_{\pi^\pm/K^\pm}(\mathrm{on})$, a match between the reconstructed $\pi^\pm/K^\pm$ candidates and truth-level $\pi^\pm/K^\pm$ mesons is performed instead of applying the PID on the MC sample. The reconstructed $\pi^\pm/K^\pm$ candidate is matched with a truth-level $\pi^\pm/K^\pm$ meson if the opening angle (match angle) between their momenta is the smallest and less than 5°.

The sources of the systematic uncertainty in this analysis are categorized into two groups: those associated with the correction factor $f_{\pi^\pm/K^\pm}$, such as the MC model and the requirement of the match angle, and those related to the experimental observable $N^{\mathrm{obs}}_{\pi^\pm/K^\pm}/N^{\mathrm{obs}}_{\mathrm{had}}$, including the PID efficiency matrix, the misidentification from electrons and muons, and the hadronic event selection.

The dominant systematic uncertainty in this analysis is introduced by the MC simulation model of the inclusive hadronic events. The generated fractions of the exclusive processes containing $\pi^\pm$ and $K^\pm$, which make up the signal processes $e^+e^- \to \pi^\pm/K^\pm + X$, directly affect the correction factors $f_{\pi^\pm}$ and $f_{K^\pm}$. To investigate the corresponding uncertainty, the HYBRID model [13,25,26] is used as an alternative to simulate the inclusive hadronic events and reevaluate the correction factors. In the HYBRID model, by taking the corresponding measured cross sections and production mechanisms into account, much knowledge of the allowed exclusive processes in the BESIII energy region is implemented. The relative differences of the correction factors obtained with the nominal and alternative MC models are regarded as systematic uncertainties. Higher uncertainties in the higher-momentum region are observed, which are due to the different production cross sections and intermediate kinematics of some few-body exclusive channels containing $\pi^\pm$ and $K^\pm$ between the two models. The systematic uncertainty due to the match angle requirement is estimated by varying the acceptance threshold from 5° to 10°.

To estimate the systematic uncertainty arising from the PID efficiency matrix, a MC sampling method is applied. Since electrons and muons could also be produced in the decay of some unstable intermediate hadrons, their contributions to the raw counts through misidentification should be considered. To evaluate this contribution, we first employ the same angle match method, as used in the extraction of $\bar{N}^{\mathrm{obs}}_{\pi^\pm/K^\pm}$, to determine the number of observed $e^\pm/\mu^\pm$ in the LUARLW MC sample. Then, the PID requirements are applied on the observed $e^\pm/\mu^\pm$ to determine their contributions to $N^{\mathrm{raw}}_{\pi^\pm/K^\pm}$. After normalization based on the luminosity of the data, these contributions are subtracted from the nominal $N^{\mathrm{raw}}_{\pi^\pm/K^\pm}$, and the resulting relative deviations in $N^{\mathrm{obs}}_{\pi^\pm/K^\pm}$ are taken as the systematic uncertainties. The uncertainty due to the imperfect simulation of various kinematic variables for the signal events is estimated by independently varying each selection criterion, increasing or decreasing it by 1 standard deviation of its resolution from the nominal value. The maximum changes of the normalized differential cross sections are regarded as the systematic uncertainties. All these individual systematic uncertainties are regarded as uncorrelated with each other and therefore are summed in quadrature. The numbers are summarized in Supplemental Material [27].

The normalized differential cross section for the inclusive $\pi^\pm$ and $K^\pm$ production in $e^+e^-$ annihilation at eight c.m. energies are shown in Fig. 1 and tabulated in Supplemental Material [27]. A new global data fit is performed for $\pi^\pm$ and $K^\pm$ FFs at next-to-next-to-leading

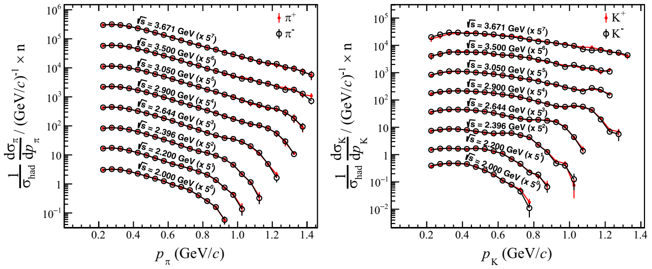

FIG. 1. Normalized differential cross sections of $e^+e^- \to \pi^\pm + X$ and $e^+e^- \to K^\pm + X$. The points with error bars are the measured values, where the uncertainties are the quadrature sum of the corresponding statistical and systematic uncertainties. Note that the observable has been scaled by an artificial factor in the plots, and the line through the bin center is to group the points according to their center-of-mass energy. The cross section of the process $e^+e^- \to K^\pm + X$ exhibits enhancements in the high-momentum regions. These enhancements may be attributed to contributions from the process $e^+e^- \to K_2^{*\pm}(1430)K^\mp$, $K_1^\pm(1400)K^\mp$, $K_1^\pm(1270)K^\mp$ [31,32].

order (NNLO) under the Nonperturbative Physics Collaboration (NPC) framework [2,28] by incorporating existing SIA world data [2] and our new results. The same parametrizations for FFs as in Ref. [2] are adopted. We have assumed charge conjugation symmetry and flavor symmetries among favored (unfavored) quark FFs as in Ref. [2]. Taking $\pi^+$ FFs as examples, we have assumed the charge conjugation symmetry $D_q^{\pi^+}(z, Q) = D_{\bar{q}}^{\pi^-}(z, Q)$ for all scale $Q$, and flavor symmetries at the starting scale $Q_0$ among favored quark FFs $D_u^{\pi^+}(z, Q_0) = D_{\bar{d}}^{\pi^+}(z, Q_0)$ and unfavored quark FFs $D_{\bar{u}}^{\pi^+}(z, Q_0) = D_d^{\pi^+}(z, Q_0)$, $D_s^{\pi^+}(z, Q_0) = D_{\bar{s}}^{\pi^+}(z, Q_0)$. Because of the limitation of pure SIA data, we have applied an additional constraint that the $s$ quark FF shares the same shape as the $\bar{u}$ quark FF at the starting scale $Q_0$. This results in a total of 26 and 24 free parameters for $\pi^\pm$ and $K^\pm$ FFs, respectively. To ensure the validity of factorization and perturbative QCD (pQCD) calculations, only the results satisfying $\sqrt{s} > 3$ GeV and $E_h > 0.8$ GeV for BESIII measurements are employed in the fit. Figure 2 illustrates the comparison between the experimental results and the fit at 3.050 and 3.671 GeV. The overall $\chi^2/N_{pt}$ values are $294.5/365 = 0.81$ and $230.5/343 = 0.67$ for $\pi^\pm$, $K^\pm$, respectively, while those for BESIII $\pi^\pm$ and $K^\pm$ data are $73.4/76 = 0.97$ and $67.2/76 = 0.88$, respectively. As shown by the green and red bands for $\pi^\pm$ and $K^\pm$, respectively, the fitting results based on the newly extracted FFs can reasonably well explain the data in regions where BESIII data are included in the global analysis. This indicates the validity of QCD factorization and fixed-order pQCD calculations at

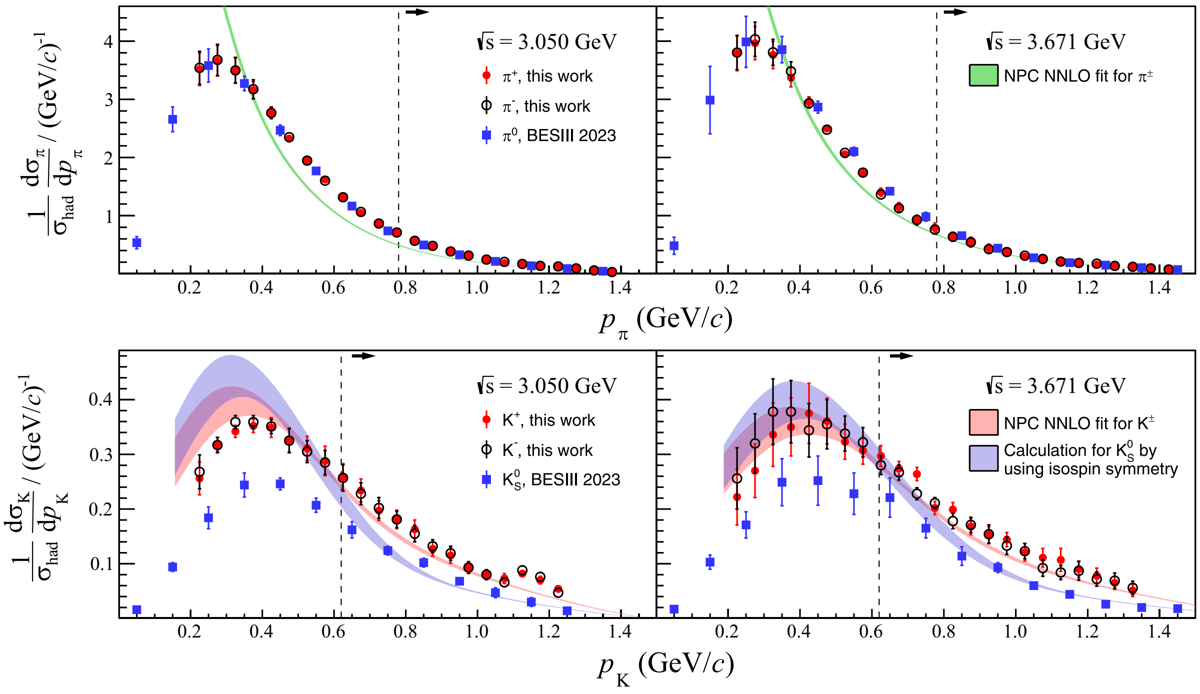

FIG. 2. Normalized differential cross sections of $e^+e^- \to \pi^\pm + X$ and $e^+e^- \to K^\pm + X$. The points with error bars are the measured values, where the uncertainties are the quadrature sum of the corresponding statistical and systematic uncertainties. The $\pi^0$ and $K_S^0$ results at the same center-of-mass energies from previous measurements at BESIII [33] are also shown. The green and red bands denote the "NPC" NNLO calculations [2,28] with $1\sigma$ limits, based on new global analyses by including SIA world data [2] and our new results. The blue band is the "NPC" NNLO calculation for $K_S^0$ by using $K^\pm$ fragmentation functions via isospin symmetry. Only the measurements on the right of the dotted lines are employed in the fit.

energy scales $\sqrt{s}$ down to 3 GeV. In the low-momentum region, however, the data exhibit discrepancies compared to theoretical predictions from fixed-order pQCD calculations. This discrepancy arises primarily due to small $z$-logarithmic enhancements and higher-twist contributions, which become increasingly relevant in this regime [29,30] and are not included in the NPC fits based on NNLO calculations. Our results in this region provide valuable new inputs for advancing theoretical investigations in QCD.

The combination of the new $\pi^{\pm}$, $K^{\pm}$ and the previous $\pi^0$, $K_S^0$ measurements at BESIII [33] allows for a test of the isospin symmetry. The measurements of the neutral pion and kaon were conducted independently, strategically taking advantage of $\pi^0 \to \gamma\gamma$ and $K_S^0 \to \pi^+\pi^-$ decay processes, thereby avoiding misidentification of signals. As shown in Fig. 2, the measured $\pi^{\pm}$ cross sections are consistent with those of $\pi^0$, indicating isospin symmetry in the hadronization process of pion production, which can be expressed in terms of the FFs as $D_i^{\pi^0} = \frac{1}{2}(D_i^{\pi^+} + D_i^{\pi^-})$ for any parton $i$. However, the measured $K^{\pm}$ cross sections are systematically higher than those of $K_S^0$. To understand the yield difference between $K^{\pm}$ and $K_S^0$, we start with the new $K^{\pm}$ FFs extraction mentioned above, from which we form a new set of $K_S^0$ FFs via SU(2) isospin symmetry. The isospin symmetry of $K_S^0$ and $K^{\pm}$ FFs has been used in global analyses of kaon FFs [29,34], and reads $D_q^{K_S^0} = \frac{1}{2}(D_{q'}^{K^+} + D_{q'}^{K^-})$, with $q' = u,\ d$ if $q = d,\ u$, otherwise $q = q'$. Utilizing the derived $K_S^0$ FFs, theoretical predictions on the $K_S^0$ yield are made, as illustrated by the blue band in Fig. 2, and show consistency with the BESIII $K_S^0$ results in kinematic regions where the $K^{\pm}$ FFs fit is performed. This provides the first support for isospin symmetry at energy scales below 10 GeV in $\pi^{\pm}/\pi^0$ and $K^{\pm}/K_S^0$ fragmentation processes. The yield difference between $K^{\pm}$ and $K_S^0$ is mainly due to the exchange of $u$ and $d$ quark FFs while applying the isospin symmetry, in contrast with the pion case.

In summary, we have measured the normalized differential cross sections of the $e^+e^- \to \pi^{\pm}/K^{\pm} + X$ processes using data samples collected from $\sqrt{s} = 2.000$ to 3.671 GeV, with $z$ coverage from 0.13 to 0.95 and from 0.30 to 0.95 for $\pi^{\pm}$ and $K^{\pm}$, respectively. The data precision can reach around 1(2)% at $z \sim 0.3$–$0.5$ for $\pi^{\pm}$ ($K^{\pm}$). The QCD-based analyses at NNLO under the NPC framework show that, in particular momentum regions, the data can be described reasonably well by pQCD calculations at energy scales down to 3 GeV using extracted FFs. The $\pi^{\pm}$ yield aligns well with a set of independent $\pi^0$ measurements at BESIII [33]. At $E_h > 0.8$ GeV, although a higher $K^{\pm}$ production cross section is observed compared to that of $K_S^0$ production, our Letter supports the isospin symmetry in parton fragmentation processes. Our results fill a particular energy region where sparse inclusive charged hadron SIA data have been reported before. They provide new ingredients for future FF global data fits, thereby enhancing our understanding of hadronization in the relatively low-energy region.

*Acknowledgments*—The BESIII Collaboration thanks the staff of BEPCII [35] and the IHEP computing center for their strong support. This work is supported in part by National Key R&D Program of China under Contracts No. 2023YFA1606000, No. 2023YFA1606704, and No. 2023YFA1609400; National Natural Science Foundation of China (NSFC) under Contracts No. 11635010, No. 11735014, No. 11935015, No. 11935016, No. 11935018, No. 12025502, No. 12035009, No. 12035013, No. 12061131003, No. 12192260, No. 12192261, No. 12192262, No. 12192263, No. 12192264, No. 12192265, No. 12221005, No. 12225509, No. 12235017, No. 12361141819, No. 12475139, No. 12205255, No. 12525508, and No. 12275173; the Chinese Academy of Sciences (CAS) Large-Scale Scientific Facility Program; the CAS Center for Excellence in Particle Physics; the Southern Center for Nuclear-Science Theory; CAS Project for Young Scientists in Basic Research under Contract No. YSBR-117; Joint Large-Scale Scientific Facility Funds of the NSFC and CAS under Contracts No. U1832207, No. U1732263, and No. U2032105; CAS under Contract No. YSBR-101; 100 Talents Program of CAS; Postdoctoral Fellowship Program and China Postdoctoral Science Foundation under Grant No. GZC20252206; Natural Science Foundation of Gansu Province under Contract No. 23JRRA578; The Institute of Nuclear and Particle Physics and Shanghai Key Laboratory for Particle Physics and Cosmology; Agencia Nacional de Investigación y Desarrollo de Chile (ANID), Chile under Contract No. ANID PIA/APOYO AFB230003; German Research Foundation DFG under Contract No. FOR5327; Istituto Nazionale di Fisica Nucleare, Italy; Knut and Alice Wallenberg Foundation under Contracts No. 2021.0174 and No. 2021.0299; Ministry of Development of Turkey under Contract No. DPT2006K-120470; National Research Foundation of Korea under Contract No. NRF-2022R1A2C1092335; National Science and Technology fund of Mongolia; National Science Research and Innovation Fund via the Program Management Unit for Human Resources & Institutional Development, Research and Innovation of Thailand under Contract No. B50G670107; Polish National Science Centre under Contract No. 2019/35/O/ST2/02907; Swedish Research Council under Contract No. 2019.04595; The Swedish

Foundation for International Cooperation in Research and Higher Education under Contract No. CH2018-7756; U.S. Department of Energy under Contract No. DE-FG02-05ER41374.

*Data availability*—The data are not publicly available. The data are available from the authors upon reasonable request.

[1] J. C. Collins, D. E. Soper, and G. F. Sterman, Factorization of hard processes in QCD, Adv. Ser. Dir. High Energy Phys. **5**, 1 (1989).

[2] J. Gao, C. Liu, X. Shen, H. Xing, and Y. Zhao, Global analysis of fragmentation functions to charged hadrons with high-precision data from the LHC, Phys. Rev. D **110**, 114019 (2024).

[3] M. Leitgab *et al.* (Belle Collaboration), Precision measurement of charged pion and kaon differential cross sections in $e^+e^-$ annihilation at $\sqrt{s} = 10.52$ GeV, Phys. Rev. Lett. **111**, 062002 (2013).

[4] R. Seidl *et al.* (Belle Collaboration), Production cross sections of light and charmed mesons in $e^+e^-$ annihilation near 10.58 GeV, Phys. Rev. D **111**, 052003 (2025).

[5] J. P. Lees *et al.* (*BABAR* Collaboration), Production of charged pions, kaons, and protons in $e^+e^-$ annihilations into hadrons at $\sqrt{s} = 10.54$ GeV, Phys. Rev. D **88**, 032011 (2013).

[6] R. Brandelik *et al.* (DASP Collaboration), Charged pion, kaon and nucleon production by $e^+e^-$ annihilation for c.m. energies between 3.6 GeV and 5.2 GeV, Nucl. Phys. **B148**, 189 (1979).

[7] G. D. Alexeev *et al.*, Multiplicities of positive and negative pions, kaons and unidentified hadrons from deep-inelastic scattering of muons off a liquid hydrogen target, Phys. Rev. D **112**, 012002 (2025).

[8] A. Airapetian *et al.* (HERMES Collaboration), Multiplicities of charged pions and kaons from semi-inclusive deep-inelastic scattering by the proton and the deuteron, Phys. Rev. D **87**, 074029 (2013).

[9] Y. X. Zhao *et al.* (Jefferson Lab Hall A Collaboration), Single spin asymmetries in charged kaon production from semi-inclusive deep inelastic scattering on a transversely polarized $^3$He target, Phys. Rev. C **90**, 055201 (2014).

[10] H. Adhikary *et al.* (NA61/SHINE Collaboration), Evidence of isospin-symmetry violation in high-energy collisions of atomic nuclei, Nat. Commun. **16**, 2849 (2025).

[11] M. Ablikim *et al.* (BESIII Collaboration), Design and construction of the BESIII detector, Nucl. Instrum. Methods Phys. Res., Sect. A **614**, 345 (2010).

[12] C. Yu *et al.*, BEPCII performance and beam dynamics studies on luminosity, in *Proceedings of the 7th International Particle Accelerator Conference* (JACoW, Geneva, Switzerland, 2016), TUYA01.

[13] M. Ablikim *et al.* (BESIII Collaboration), Measurement of the cross section for $e^+e^- \to$ hadrons at energies from 2.2324 to 3.6710 GeV, Phys. Rev. Lett. **128**, 062004 (2022).

[14] S. Agostinelli *et al.* (GEANT4 Collaboration), Geant4–A simulation toolkit, Nucl. Instrum. Methods Phys. Res., Sect. A **506**, 250 (2003).

[15] C. M. Carloni Calame, C. Lunardini, G. Montagna, O. Nicrosini, and F. Piccinini, Large angle Bhabha scattering and luminosity at flavor factories, Nucl. Phys. **B584**, 459 (2000).

[16] S. Jadach, B. F. L. Ward, and Z. Was, The precision Monte Carlo event generator K K for two fermion final states in $e^+e^-$ collisions, Comput. Phys. Commun. **130**, 260 (2000).

[17] D. J. Lange, The EvtGen particle decay simulation package, Nucl. Instrum. Methods Phys. Res., Sect. A **462**, 152 (2001).

[18] R. G. Ping, Event generators at BESIII, Chin. Phys. C **32**, 599 (2008).

[19] F. A. Berends, P. H. Daverveldt, and R. Kleiss, Monte Carlo simulation of two photon processes. 2. Complete lowest order calculations for four lepton production processes in electron positron collisions, Comput. Phys. Commun. **40**, 285 (1986).

[20] H. Czyż, P. Kisza, and S. Tracz, Modeling interactions of photons with pseudoscalar and vector mesons, Phys. Rev. D **97**, 016006 (2018).

[21] G. A. Schuler, Two photon physics with GALUGA 2.0, Comput. Phys. Commun. **108**, 279 (1998).

[22] The $\cos\theta$ values of these bins are around ±0.83, which correspond to the two gaps between barrel and end-cap EMC. In these bins, the Bhabha events survive the inclusive hadronic event selection criteria since they do not leave shower in EMC. Given that the fraction of these Bhabha events are less than 10% and they are reasonably simulated and subtracted, we do not further suppress them in this analysis.

[23] B. Andersson, *The Lund Model*, Cambridge Monographs on Particle Physics, Nuclear Physics and Cosmology Vol. 7 (Cambridge University Press, Cambridge, England, 2023), 10.1017/9781009401296.

[24] B. Andersson and H.-m. Hu, Few body states in Lund string fragmentation model, arXiv:hep-ph/9910285.

[25] G. Rodrigo, H. Czyz, J. H. Kuhn, and M. Szopa, Radiative return at NLO and the measurement of the hadronic cross-section in electron positron annihilation, Eur. Phys. J. C **24**, 71 (2002).

[26] R. G. Ping *et al.*, Tuning and validation of hadronic event generator for *R* value measurements in the tau-charm region, Chin. Phys. C **40**, 113002 (2016).

[27] See Supplemental Material at http://link.aps.org/supplemental/10.1103/5kxw-3mbw for a detailed listing of systematic uncertainties and the tabulated results.

[28] J. Gao, C. Liu, X. Shen, H. Xing, and Y. Zhao, Simultaneous determination of fragmentation functions and test on momentum sum rule, Phys. Rev. Lett. **132**, 261903 (2024).

[29] D. de Florian, R. Sassot, and M. Stratmann, Global analysis of fragmentation functions for pions and kaons and their uncertainties, Phys. Rev. D **75**, 114010 (2007).

[30] M. Li, D. P. Anderle, H. Xing, and Y. Zhao, Analysis of $\pi^0$, $K_S^0$ and $\eta$ fragmentation functions using single-inclusive annihilation data including BESIII measurements, Phys. Rev. D **111**, 034030 (2025).

[31] M. Ablikim *et al.* (BESIII Collaboration), Measurement of $e^+e^- \to K^+K^-\pi^0$ cross section and observation of a resonant structure, J. High Energy Phys. 07 (2022) 045.

[32] M. Ablikim *et al.* (BESIII Collaboration), Observation of a resonant structure in $e^+e^- \to K^+K^-\pi^0\pi^0$, Phys. Rev. Lett. **124**, 112001 (2020).

[33] M. Ablikim *et al.* (BESIII Collaboration), Measurements of normalized differential cross sections of inclusive $\pi^0$ and $K_S^0$ production in $e^+e^-$ annihilation at energies from 2.2324 to 3.6710 GeV, Phys. Rev. Lett. **130**, 231901 (2023).

[34] S. Albino, B. A. Kniehl, and G. Kramer, AKK update: Improvements from new theoretical input and experimental data, Nucl. Phys. **B803**, 42 (2008).

[35] https://cstr.cn/31109.02.BEPC.

M. Ablikim,[1] M. N. Achasov,[4,c] P. Adlarson,[77] X. C. Ai,[82] R. Aliberti,[36] A. Amoroso,[76a,76c] Q. An,[73,59,a] Y. Bai,[58]
O. Bakina,[37] Y. Ban,[47,h] H.-R. Bao,[65] V. Batozskaya,[1,45] K. Begzsuren,[33] N. Berger,[36] M. Berlowski,[45] M. Bertani,[29a]
D. Bettoni,[30a] F. Bianchi,[76a,76c] E. Bianco,[76a,76c] A. Bortone,[76a,76c] I. Boyko,[37] R. A. Briere,[5] A. Brueggemann,[70] H. Cai,[78]
M. H. Cai,[39,k,l] X. Cai,[1,59] A. Calcaterra,[29a] G. F. Cao,[1,65] N. Cao,[1,65] S. A. Cetin,[63a] X. Y. Chai,[47,h] J. F. Chang,[1,59]
G. R. Che,[44] Y. Z. Che,[1,59,65] G. Chelkov,[37,b] C. H. Chen,[9] Chao Chen,[56] G. Chen,[1] H. S. Chen,[1,65] H. Y. Chen,[21]
M. L. Chen,[1,59,65] S. J. Chen,[43] S. L. Chen,[46] S. M. Chen,[62] T. Chen,[1,65] X. R. Chen,[32,65] X. T. Chen,[1,65] X. Y. Chen,[12,g]
Y. B. Chen,[1,59] Y. Q. Chen,[35] Y. Q. Chen,[16] Z. J. Chen,[26,i] Z. K. Chen,[60] S. K. Choi,[10] X. Chu,[12,g] G. Cibinetto,[30a]
F. Cossio,[76c] J. Cottee-Meldrum,[64] J. J. Cui,[51] H. L. Dai,[1,59] J. P. Dai,[80] A. Dbeyssi,[19] R. E. de Boer,[3] D. Dedovich,[37]
C. Q. Deng,[74] Z. Y. Deng,[1] A. Denig,[36] I. Denysenko,[37] M. Destefanis,[76a,76c] F. De Mori,[76a,76c] B. Ding,[68,1] X. X. Ding,[47,h]
Y. Ding,[41] Y. Ding,[35] Y. X. Ding,[31] J. Dong,[1,59] L. Y. Dong,[1,65] M. Y. Dong,[1,59,65] X. Dong,[78] M. C. Du,[1] S. X. Du,[82]
S. X. Du,[12,g] Y. Y. Duan,[56] Z. H. Duan,[43] P. Egorov,[37,b] G. F. Fan,[43] J. J. Fan,[20] Y. H. Fan,[46] J. Fang,[60] J. Fang,[1,59]
S. S. Fang,[1,65] W. X. Fang,[1] Y. Q. Fang,[1,59] R. Farinelli,[30a] L. Fava,[76b,76c] F. Feldbauer,[3] G. Felici,[29a] C. Q. Feng,[73,59]
J. H. Feng,[16] L. Feng,[39,k,l] Q. X. Feng,[39,k,l] Y. T. Feng,[73,59] M. Fritsch,[3] C. D. Fu,[1] J. L. Fu,[65] Y. W. Fu,[1,65] H. Gao,[65] J. Gao,[52]
X. B. Gao,[42] Y. Gao,[73,59] Y. N. Gao,[47,h] Y. N. Gao,[20] Y. Y. Gao,[31] S. Garbolino,[76c] I. Garzia,[30a,30b] L. Ge,[58] P. T. Ge,[20]
Z. W. Ge,[43] C. Geng,[60] E. M. Gersabeck,[69] A. Gilman,[71] K. Goetzen,[13] J. D. Gong,[35] L. Gong,[41] W. X. Gong,[1,59] W. Gradl,[36]
S. Gramigna,[30a,30b] M. Greco,[76a,76c] M. H. Gu,[1,59] Y. T. Gu,[15] C. Y. Guan,[1,65] A. Q. Guo,[32] L. B. Guo,[42] M. J. Guo,[51]
R. P. Guo,[50] Y. P. Guo,[12,g] A. Guskov,[37,b] J. Gutierrez,[28] K. L. Han,[65] T. T. Han,[1] F. Hanisch,[3] K. D. Hao,[73,59] X. Q. Hao,[20]
F. A. Harris,[67] K. K. He,[56] K. L. He,[1,65] F. H. Heinsius,[3] C. H. Heinz,[36] Y. K. Heng,[1,59,65] C. Herold,[61] T. Holtmann,[3]
P. C. Hong,[35] G. Y. Hou,[1,65] X. T. Hou,[1,65] Y. R. Hou,[65] Z. L. Hou,[1] H. M. Hu,[1,65] J. F. Hu,[57,j] Q. P. Hu,[73,59] S. L. Hu,[12,g]
T. Hu,[1,59,65] Y. Hu,[1] Z. M. Hu,[60] G. S. Huang,[73,59] K. X. Huang,[60] L. Q. Huang,[32,65] P. Huang,[43] X. T. Huang,[51] Y. P. Huang,[1]
Y. S. Huang,[60] T. Hussain,[75] N. Hüsken,[36] N. in der Wiesche,[70] J. Jackson,[28] Q. Ji,[1] Q. P. Ji,[20] W. Ji,[1,65] X. B. Ji,[1,65]
X. L. Ji,[1,59] Y. Y. Ji,[51] Z. K. Jia,[73,59] D. Jiang,[1,65] H. B. Jiang,[78] P. C. Jiang,[47,h] S. J. Jiang,[9] T. J. Jiang,[17] X. S. Jiang,[1,59,65]
Y. Jiang,[65] J. B. Jiao,[51] J. K. Jiao,[35] Z. Jiao,[24] S. Jin,[43] Y. Jin,[68] M. Q. Jing,[1,65] X. M. Jing,[65] T. Johansson,[77] S. Kabana,[34]
N. Kalantar-Nayestanaki,[66] X. L. Kang,[9] X. S. Kang,[41] M. Kavatsyuk,[66] B. C. Ke,[82] V. Khachatryan,[28] A. Khoukaz,[70]
R. Kiuchi,[1] O. B. Kolcu,[63a] B. Kopf,[3] M. Kuessner,[3] X. Kui,[1,65] N. Kumar,[27] A. Kupsc,[45,77] W. Kühn,[38] Q. Lan,[74]
W. N. Lan,[20] T. T. Lei,[73,59] M. Lellmann,[36] T. Lenz,[36] C. Li,[48] C. Li,[44] C. Li,[73,59] C. H. Li,[40] C. K. Li,[21] D. M. Li,[82] F. Li,[1,59]
G. Li,[1] H. B. Li,[1,65] H. J. Li,[20] H. N. Li,[57,j] Hui Li,[44] J. R. Li,[62] J. S. Li,[60] K. Li,[1] K. L. Li,[39,k,l] K. L. Li,[20] L. J. Li,[1,65] Lei Li,[49]
M. H. Li,[44] M. R. Li,[1,65] P. L. Li,[65] P. R. Li,[39,k,l] Q. M. Li,[1,65] Q. X. Li,[51] R. Li,[18,32] S. X. Li,[12] T. Li,[51] T. Y. Li,[44] W. D. Li,[1,65]
W. G. Li,[1,a] X. Li,[1,65] X. H. Li,[73,59] X. L. Li,[51] X. Y. Li,[1,8] X. Z. Li,[60] Y. Li,[20] Y. G. Li,[47,h] Y. P. Li,[35] Z. J. Li,[60] Z. Y. Li,[80]
C. Liang,[43] H. Liang,[73,59] Y. F. Liang,[55] Y. T. Liang,[32,65] G. R. Liao,[14] L. B. Liao,[60] M. H. Liao,[60] Y. P. Liao,[1,65] J. Libby,[27]
A. Limphirat,[61] C. C. Lin,[56] C. X. Lin,[65] D. X. Lin,[32,65] L. Q. Lin,[40] T. Lin,[1] B. J. Liu,[1] B. X. Liu,[78] C. Liu,[35] C. X. Liu,[1]
F. Liu,[1] F. H. Liu,[54] Feng Liu,[6] G. M. Liu,[57,j] H. Liu,[39,k,l] H. B. Liu,[15] H. H. Liu,[1] H. M. Liu,[1,65] Huihui Liu,[22] J. B. Liu,[73,59]
J. J. Liu,[21] K. Liu,[74] K. Liu,[39,k,l] K. Y. Liu,[41] Ke Liu,[23] L. Liu,[73,59] L. C. Liu,[44] Lu Liu,[44] M. H. Liu,[12,g] P. L. Liu,[1] Q. Liu,[65]
S. B. Liu,[73,59] T. Liu,[12,g] W. K. Liu,[44] W. M. Liu,[73,59] W. T. Liu,[40] X. Liu,[40] X. Liu,[39,k,l] X. K. Liu,[39,k,l] X. Y. Liu,[78] Y. Liu,[82]
Y. Liu,[82] Y. Liu,[39,k,l] Y. B. Liu,[44] Z. A. Liu,[1,59,65] Z. D. Liu,[9] Z. Q. Liu,[51] X. C. Lou,[1,59,65] F. X. Lu,[60] H. J. Lu,[24] J. G. Lu,[1,59]
X. L. Lu,[16] Y. Lu,[7] Y. H. Lu,[1,65] Y. P. Lu,[1,59] Z. H. Lu,[1,65] C. L. Luo,[42] J. R. Luo,[60] J. S. Luo,[1,65] M. X. Luo,[81] T. Luo,[12,g]
X. L. Luo,[1,59] Z. Y. Lv,[23] X. R. Lyu,[65,p] Y. F. Lyu,[44] Y. H. Lyu,[82] F. C. Ma,[41] H. Ma,[80] H. L. Ma,[1] J. L. Ma,[1,65] L. L. Ma,[51]
L. R. Ma,[68] Q. M. Ma,[1] R. Q. Ma,[1,65] R. Y. Ma,[20] T. Ma,[73,59] X. T. Ma,[1,65] X. Y. Ma,[1,59] Y. M. Ma,[32] F. E. Maas,[19]
I. MacKay,[71] M. Maggiora,[76a,76c] S. Malde,[71] Q. A. Malik,[75] H. X. Mao,[39,k,l] Y. J. Mao,[47,h] Z. P. Mao,[1] S. Marcello,[76a,76c]

A. Marshall,[64] F. M. Melendi,[30a,30b] Y. H. Meng,[65] Z. X. Meng,[68] J. G. Messchendorp,[13,66] G. Mezzadri,[30a] H. Miao,[1,65]
T. J. Min,[43] R. E. Mitchell,[28] X. H. Mo,[1,59,65] B. Moses,[28] N. Yu. Muchnoi,[4,c] J. Muskalla,[36] Y. Nefedov,[37] F. Nerling,[19,e]
L. S. Nie,[21] I. B. Nikolaev,[4,c] Z. Ning,[1,59] S. Nisar,[11,m] Q. L. Niu,[39,k,l] W. D. Niu,[12,g] C. Normand,[64] S. L. Olsen,[10,65]
Q. Ouyang,[1,59,65] S. Pacetti,[29b,29c] X. Pan,[56] Y. Pan,[58] A. Pathak,[10] Y. P. Pei,[73,59] M. Pelizaeus,[3] H. P. Peng,[73,59] X. J. Peng,[39,k,l]
Y. Y. Peng,[39,k,l] K. Peters,[13,e] K. Petridis,[64] J. L. Ping,[42] R. G. Ping,[1,65] S. Plura,[36] V. Prasad,[34] F. Z. Qi,[1] H. R. Qi,[62] M. Qi,[43]
S. Qian,[1,59] W. B. Qian,[65] C. F. Qiao,[65] J. H. Qiao,[20] J. J. Qin,[74] J. L. Qin,[56] L. Q. Qin,[14] L. Y. Qin,[73,59] P. B. Qin,[74]
X. P. Qin,[12,g] X. S. Qin,[51] Z. H. Qin,[1,59] J. F. Qiu,[1] Z. H. Qu,[74] J. Rademacker,[64] C. F. Redmer,[36] A. Rivetti,[76c] M. Rolo,[76c]
G. Rong,[1,65] S. S. Rong,[1,65] F. Rosini,[29b,29c] Ch. Rosner,[19] M. Q. Ruan,[1,59] N. Salone,[45] A. Sarantsev,[37,d] Y. Schelhaas,[36]
K. Schoenning,[77] M. Scodeggio,[30a] K. Y. Shan,[12,g] W. Shan,[25] X. Y. Shan,[73,59] Z. J. Shang,[39,k,l] J. F. Shangguan,[17]
L. G. Shao,[1,65] M. Shao,[73,59] C. P. Shen,[12,g] H. F. Shen,[1,8] W. H. Shen,[65] X. M. Shen,[32,52,65] X. Y. Shen,[1,65] B. A. Shi,[65]
H. Shi,[73,59] J. L. Shi,[12,g] J. Y. Shi,[1] S. Y. Shi,[74] X. Shi,[1,59] H. L. Song,[73,59] J. J. Song,[20] T. Z. Song,[60] W. M. Song,[35]
Y. J. Song,[12,g] Y. X. Song,[47,h,n] S. Sosio,[76a,76c] S. Spataro,[76a,76c] F. Stieler,[36] S. S. Su,[41] Y. J. Su,[65] G. B. Sun,[78] G. X. Sun,[1]
H. Sun,[65] H. K. Sun,[1] J. F. Sun,[20] K. Sun,[62] L. Sun,[78] S. S. Sun,[1,65] T. Sun,[52,f] Y. C. Sun,[78] Y. H. Sun,[31] Y. J. Sun,[73,59]
Y. Z. Sun,[1] Z. Q. Sun,[1,65] Z. T. Sun,[51] C. J. Tang,[55] G. Y. Tang,[1] J. Tang,[60] J. J. Tang,[73,59] L. F. Tang,[40] Y. A. Tang,[78]
L. Y. Tao,[74] M. Tat,[71] J. X. Teng,[73,59] J. Y. Tian,[73,59] W. H. Tian,[60] Y. Tian,[32] Z. F. Tian,[78] I. Uman,[63b] B. Wang,[60] B. Wang,[1]
Bo Wang,[73,59] C. Wang,[39,k,l] C. Wang,[20] Cong Wang,[23] D. Y. Wang,[47,h] H. J. Wang,[39,k,l] J. J. Wang,[78] K. Wang,[1,59]
L. L. Wang,[1] L. W. Wang,[35] M. Wang,[51] M. Wang,[73,59] N. Y. Wang,[65] S. Wang,[12,g] T. Wang,[12,g] T. J. Wang,[44] W. Wang,[74]
W. Wang,[60] W. P. Wang,[36,o] X. Wang,[47,h] X. F. Wang,[39,k,l] X. J. Wang,[40] X. L. Wang,[12,g] X. N. Wang,[1] Y. Wang,[62]
Y. D. Wang,[46] Y. F. Wang,[1,59,65] Y. H. Wang,[39,k,l] Y. J. Wang,[73,59] Y. L. Wang,[20] Y. N. Wang,[78] Y. Q. Wang,[1] Yaqian Wang,[18]
Yi Wang,[62] Yuan Wang,[18,32] Z. Wang,[1,59] Z. L. Wang,[2] Z. L. Wang,[74] Z. Q. Wang,[12,g] Z. Y. Wang,[1,65] D. H. Wei,[14]
H. R. Wei,[44] F. Weidner,[70] S. P. Wen,[1] Y. R. Wen,[40] U. Wiedner,[3] G. Wilkinson,[71] M. Wolke,[77] C. Wu,[40] J. F. Wu,[1,8]
L. H. Wu,[1] L. J. Wu,[1,65] L. J. Wu,[20] Lianjie Wu,[20] S. G. Wu,[1,65] S. M. Wu,[65] X. Wu,[12,g] X. H. Wu,[35] Y. J. Wu,[32] Z. Wu,[1,59]
L. Xia,[73,59] X. M. Xian,[40] B. H. Xiang,[1,65] D. Xiao,[39,k,l] G. Y. Xiao,[43] H. Xiao,[74] Y. L. Xiao,[12,g] Z. J. Xiao,[42] C. Xie,[43]
K. J. Xie,[1,65] X. H. Xie,[47,h] Y. Xie,[51] Y. G. Xie,[1,59] Y. H. Xie,[6] Z. P. Xie,[73,59] H. X. Xing,[57,j] T. Y Xing,[1,65] C. F. Xu,[1,65]
C. J. Xu,[60] G. F. Xu,[1] H. Y. Xu,[2] H. Y. Xu,[68,2] M. Xu,[73,59] Q. J. Xu,[17] Q. N. Xu,[31] T. D. Xu,[74] W. Xu,[1] W. L. Xu,[68] X. P. Xu,[56]
Y. Xu,[41] Y. Xu,[12,g] Y. C. Xu,[79] Z. S. Xu,[65] F. Yan,[12,g] H. Y. Yan,[40] L. Yan,[12,g] W. B. Yan,[73,59] W. C. Yan,[82] W. H. Yan,[6]
W. P. Yan,[20] X. Q. Yan,[1,65] H. J. Yang,[52,f] H. L. Yang,[35] H. X. Yang,[1] J. H. Yang,[43] R. J. Yang,[20] T. Yang,[1] Y. Yang,[12,g]
Y. F. Yang,[44] Y. H. Yang,[43] Y. Q. Yang,[9] Y. X. Yang,[1,65] Y. Z. Yang,[20] M. Ye,[1,59] M. H. Ye,[8] Z. J. Ye,[57,j] Junhao Yin,[44]
Z. Y. You,[60] B. X. Yu,[1,59,65] C. X. Yu,[44] G. Yu,[13] J. S. Yu,[26,i] L. Q. Yu,[12,g] M. C. Yu,[41] T. Yu,[74] X. D. Yu,[47,h] Y. C. Yu,[82]
C. Z. Yuan,[1,65] H. Yuan,[1,65] J. Yuan,[46] J. Yuan,[35] L. Yuan,[2] S. C. Yuan,[1,65] X. Q. Yuan,[1] Y. Yuan,[1,65] Z. Y. Yuan,[60] C. X. Yue,[40]
Ying Yue,[20] A. A. Zafar,[75] S. H. Zeng,[64] X. Zeng,[12,g] Y. Zeng,[26,i] Y. J. Zeng,[60] Y. J. Zeng,[1,65] X. Y. Zhai,[35] Y. H. Zhan,[60]
A. Q. Zhang,[1,65] B. L. Zhang,[1,65] B. X. Zhang,[1] D. H. Zhang,[44] G. Y. Zhang,[20] G. Y. Zhang,[1,65] H. Zhang,[82] H. Zhang,[73,59]
H. C. Zhang,[1,59,65] H. H. Zhang,[60] H. Q. Zhang,[1,59,65] H. R. Zhang,[73,59] H. Y. Zhang,[1,59] J. Zhang,[82] J. Zhang,[60] J. J. Zhang,[53]
J. L. Zhang,[21] J. Q. Zhang,[42] J. S. Zhang,[12,g] J. W. Zhang,[1,59,65] J. X. Zhang,[39,k,l] J. Y. Zhang,[1] J. Z. Zhang,[1,65]
Jianyu Zhang,[65] L. M. Zhang,[62] Lei Zhang,[43] N. Zhang,[82] P. Zhang,[1,65] Q. Zhang,[20] Q. Y. Zhang,[35] R. Y. Zhang,[39,k,l]
S. H. Zhang,[1,65] Shulei Zhang,[26,i] X. M. Zhang,[1] X. Y. Zhang,[41] X. Y. Zhang,[51] Y. Zhang,[1] Y. Zhang,[74] Y. T. Zhang,[82]
Y. H. Zhang,[1,59] Y. M. Zhang,[40] Y. P. Zhang,[73,59] Z. D. Zhang,[1] Z. H. Zhang,[1] Z. L. Zhang,[35] Z. L. Zhang,[56] Z. X. Zhang,[20]
Z. Y. Zhang,[44] Z. Y. Zhang,[78] Z. Z. Zhang,[46] Zh. Zh. Zhang,[20] G. Zhao,[1] J. Y. Zhao,[1,65] J. Z. Zhao,[1,59] L. Zhao,[73,59] L. Zhao,[1]
M. G. Zhao,[44] N. Zhao,[80] R. P. Zhao,[65] S. J. Zhao,[82] Y. B. Zhao,[1,59] Y. L. Zhao,[56] Y. X. Zhao,[32,65] Z. G. Zhao,[73,59]
A. Zhemchugov,[37,b] B. Zheng,[74] B. M. Zheng,[35] J. P. Zheng,[1,59] W. J. Zheng,[1,65] X. R. Zheng,[20] Y. H. Zheng,[65,p] B. Zhong,[42]
C. Zhong,[20] H. Zhou,[36,51,o] J. Q. Zhou,[35] J. Y. Zhou,[35] S. Zhou,[6] X. Zhou,[78] X. K. Zhou,[6] X. R. Zhou,[73,59] X. Y. Zhou,[40]
Y. X. Zhou,[79] Y. Z. Zhou,[12,g] A. N. Zhu,[65] J. Zhu,[44] K. Zhu,[1] K. J. Zhu,[1,59,65] K. S. Zhu,[12,g] L. Zhu,[35] L. X. Zhu,[65]
S. H. Zhu,[72] T. J. Zhu,[12,g] W. D. Zhu,[12,g] W. D. Zhu,[42] W. J. Zhu,[1] W. Z. Zhu,[20] Y. C. Zhu,[73,59] Z. A. Zhu,[1,65] X. Y. Zhuang,[44]
J. H. Zou,[1] and J. Zu[32,65]

(BESIII Collaboration)

[1]*Institute of High Energy Physics, Beijing 100049, People's Republic of China*
[2]*Beihang University, Beijing 100191, People's Republic of China*

[3]*Bochum Ruhr-University, D-44780 Bochum, Germany*
[4]*Budker Institute of Nuclear Physics SB RAS (BINP), Novosibirsk 630090, Russia*
[5]*Carnegie Mellon University, Pittsburgh, Pennsylvania 15213, USA*
[6]*Central China Normal University, Wuhan 430079, People's Republic of China*
[7]*Central South University, Changsha 410083, People's Republic of China*
[8]*China Center of Advanced Science and Technology, Beijing 100190, People's Republic of China*
[9]*China University of Geosciences, Wuhan 430074, People's Republic of China*
[10]*Chung-Ang University, Seoul, 06974, Republic of Korea*
[11]*COMSATS University Islamabad, Lahore Campus, Defence Road, Off Raiwind Road, 54000 Lahore, Pakistan*
[12]*Fudan University, Shanghai 200433, People's Republic of China*
[13]*GSI Helmholtzcentre for Heavy Ion Research GmbH, D-64291 Darmstadt, Germany*
[14]*Guangxi Normal University, Guilin 541004, People's Republic of China*
[15]*Guangxi University, Nanning 530004, People's Republic of China*
[16]*Guangxi University of Science and Technology, Liuzhou 545006, People's Republic of China*
[17]*Hangzhou Normal University, Hangzhou 310036, People's Republic of China*
[18]*Hebei University, Baoding 071002, People's Republic of China*
[19]*Helmholtz Institute Mainz, Staudinger Weg 18, D-55099 Mainz, Germany*
[20]*Henan Normal University, Xinxiang 453007, People's Republic of China*
[21]*Henan University, Kaifeng 475004, People's Republic of China*
[22]*Henan University of Science and Technology, Luoyang 471003, People's Republic of China*
[23]*Henan University of Technology, Zhengzhou 450001, People's Republic of China*
[24]*Huangshan College, Huangshan 245000, People's Republic of China*
[25]*Hunan Normal University, Changsha 410081, People's Republic of China*
[26]*Hunan University, Changsha 410082, People's Republic of China*
[27]*Indian Institute of Technology Madras, Chennai 600036, India*
[28]*Indiana University, Bloomington, Indiana 47405, USA*
[29a]*INFN Laboratori Nazionali di Frascati, I-00044, Frascati, Italy*
[29b]*INFN Sezione di Perugia, I-06100, Perugia, Italy*
[29c]*University of Perugia, I-06100, Perugia, Italy*
[30a]*INFN Sezione di Ferrara, I-44122, Ferrara, Italy*
[30b]*University of Ferrara, I-44122, Ferrara, Italy*
[31]*Inner Mongolia University, Hohhot 010021, People's Republic of China*
[32]*Institute of Modern Physics, Lanzhou 730000, People's Republic of China*
[33]*Institute of Physics and Technology, Mongolian Academy of Sciences, Peace Avenue 54B, Ulaanbaatar 13330, Mongolia*
[34]*Instituto de Alta Investigación, Universidad de Tarapacá, Casilla 7D, Arica 1000000, Chile*
[35]*Jilin University, Changchun 130012, People's Republic of China*
[36]*Johannes Gutenberg University of Mainz, Johann-Joachim-Becher-Weg 45, D-55099 Mainz, Germany*
[37]*Joint Institute for Nuclear Research, 141980 Dubna, Moscow region, Russia*
[38]*Justus-Liebig-Universitaet Giessen, II. Physikalisches Institut, Heinrich-Buff-Ring 16, D-35392 Giessen, Germany*
[39]*Lanzhou University, Lanzhou 730000, People's Republic of China*
[40]*Liaoning Normal University, Dalian 116029, People's Republic of China*
[41]*Liaoning University, Shenyang 110036, People's Republic of China*
[42]*Nanjing Normal University, Nanjing 210023, People's Republic of China*
[43]*Nanjing University, Nanjing 210093, People's Republic of China*
[44]*Nankai University, Tianjin 300071, People's Republic of China*
[45]*National Centre for Nuclear Research, Warsaw 02-093, Poland*
[46]*North China Electric Power University, Beijing 102206, People's Republic of China*
[47]*Peking University, Beijing 100871, People's Republic of China*
[48]*Qufu Normal University, Qufu 273165, People's Republic of China*
[49]*Renmin University of China, Beijing 100872, People's Republic of China*
[50]*Shandong Normal University, Jinan 250014, People's Republic of China*
[51]*Shandong University, Jinan 250100, People's Republic of China*
[52]*Shanghai Jiao Tong University, Shanghai 200240, People's Republic of China*
[53]*Shanxi Normal University, Linfen 041004, People's Republic of China*
[54]*Shanxi University, Taiyuan 030006, People's Republic of China*
[55]*Sichuan University, Chengdu 610064, People's Republic of China*
[56]*Soochow University, Suzhou 215006, People's Republic of China*
[57]*South China Normal University, Guangzhou 510006, People's Republic of China*
[58]*Southeast University, Nanjing 211100, People's Republic of China*
[59]*State Key Laboratory of Particle Detection and Electronics, Beijing 100049, Hefei 230026, People's Republic of China*

[60]*Sun Yat-Sen University, Guangzhou 510275, People's Republic of China*
[61]*Suranaree University of Technology, University Avenue 111, Nakhon Ratchasima 30000, Thailand*
[62]*Tsinghua University, Beijing 100084, People's Republic of China*
[63a]*Turkish Accelerator Center Particle Factory Group, Istinye University, 34010, Istanbul, Turkey*
[63b]*Near East University, Nicosia, North Cyprus, 99138, Mersin 10, Turkey*
[64]*University of Bristol, H H Wills Physics Laboratory, Tyndall Avenue, Bristol, BS8 1TL, United Kingdom*
[65]*University of Chinese Academy of Sciences, Beijing 100049, People's Republic of China*
[66]*University of Groningen, NL-9747 AA Groningen, The Netherlands*
[67]*University of Hawaii, Honolulu, Hawaii 96822, USA*
[68]*University of Jinan, Jinan 250022, People's Republic of China*
[69]*University of Manchester, Oxford Road, Manchester, M13 9PL, United Kingdom*
[70]*University of Muenster, Wilhelm-Klemm-Strasse 9, 48149 Muenster, Germany*
[71]*University of Oxford, Keble Road, Oxford OX13RH, United Kingdom*
[72]*University of Science and Technology Liaoning, Anshan 114051, People's Republic of China*
[73]*University of Science and Technology of China, Hefei 230026, People's Republic of China*
[74]*University of South China, Hengyang 421001, People's Republic of China*
[75]*University of the Punjab, Lahore-54590, Pakistan*
[76a]*University of Turin and INFN, I-10125, Turin, Italy*
[76b]*University of Eastern Piedmont, I-15121, Alessandria, Italy*
[76c]*INFN, I-10125, Turin, Italy*
[77]*Uppsala University, Box 516, SE-75120 Uppsala, Sweden*
[78]*Wuhan University, Wuhan 430072, People's Republic of China*
[79]*Yantai University, Yantai 264005, People's Republic of China*
[80]*Yunnan University, Kunming 650500, People's Republic of China*
[81]*Zhejiang University, Hangzhou 310027, People's Republic of China*
[82]*Zhengzhou University, Zhengzhou 450001, People's Republic of China*

[a] Deceased.

[b] Also at the Moscow Institute of Physics and Technology, Moscow 141700, Russia.

[c] Also at the Novosibirsk State University, Novosibirsk, 630090, Russia.

[d] Also at the NRC "Kurchatov Institute," PNPI, 188300, Gatchina, Russia.

[e] Also at Goethe University Frankfurt, 60323 Frankfurt am Main, Germany.

[f] Also at Key Laboratory for Particle Physics, Astrophysics and Cosmology, Ministry of Education; Shanghai Key Laboratory for Particle Physics and Cosmology; Institute of Nuclear and Particle Physics, Shanghai 200240, People's Republic of China.

[g] Also at Key Laboratory of Nuclear Physics and Ion-beam Application (MOE) and Institute of Modern Physics, Fudan University, Shanghai 200443, People's Republic of China.

[h] Also at State Key Laboratory of Nuclear Physics and Technology, Peking University, Beijing 100871, People's Republic of China.

[i] Also at School of Physics and Electronics, Hunan University, Changsha 410082, China.

[j] Also at Guangdong Provincial Key Laboratory of Nuclear Science, Institute of Quantum Matter, South China Normal University, Guangzhou 510006, China.

[k] Also at MOE Frontiers Science Center for Rare Isotopes, Lanzhou University, Lanzhou 730000, People's Republic of China.

[l] Also at Lanzhou Center for Theoretical Physics, Lanzhou University, Lanzhou 730000, People's Republic of China.

[m] Also at the Department of Mathematical Sciences, IBA, Karachi 75270, Pakistan.

[n] Also at Ecole Polytechnique Federale de Lausanne (EPFL), CH-1015 Lausanne, Switzerland.

[o] Also at Helmholtz Institute Mainz, Staudinger Weg 18, D-55099 Mainz, Germany.

[p] Also at Hangzhou Institute for Advanced Study, University of Chinese Academy of Sciences, Hangzhou 310024, China.